national accelerator laboratory

TM-473
0330

RF CAPTURE WITH ACCELERATION IN THE NAL BOOSTER

W.W. Lee and L.C. Teng

January, 1974

In the NAL booster, each rf cavity has to be turned on abruptly to avoid multi-pactoring. Computer calculations [1,2] have shown that adiabatic capture can still be accomplished in this case. For example, a completely debunched 200-MeV linac beam with $\Delta p/p = \pm 0.8 \times 10^{-3}$ can be captured completely in the rf bucket with no appreciable phase space dilution, if the voltage is turned on in 16 steps, one for each cavity, in about 160 μsec with a final voltage of 100 kV/turn. However, the capture process in a fast cycling machine, such as the booster, is accompanied by acceleration, the effects of which were ignored in previous analyses. Acceleration not only reduces the available bucket area, but destroys, to a certain degree, the adiabaticity of the process as well.[3] In this report we investigate such effects on the capture efficiency under various turn-on conditions. The method of multi-particle numerical integration is used for the study.

A. Equations for Synchrotron Motion

The motion of a particle performing synchrotron oscillations can be described by

$$\begin{cases} \dfrac{d\phi}{dt} = \omega_{rf}(t) - h\omega, & (1) \\ \dfrac{d\rho}{dt} = \dfrac{eV_{rf}(t)}{2\pi R} \sin\phi, & (2) \end{cases}$$

where

ϕ = particle rf phase,

p = particle momentum,

h = rf harmonic number,

R = particle orbit radius,

V_{rf} = rf cavity voltage,

ω_{rf} = angular frequency of rf cavity,

ω = angular frequency of particle = $c\beta/R$.

Let $\eta = \eta_s + \Delta\eta$ where $\eta_s(t)$ is the momentum in mc units of a "synchronous" particle which, corresponding to a certain prescribed guide field, maintains a constant synchronous orbit radius R_s. Other parameters associated with the synchronous particle are β_s, $\gamma_s (= \eta_s/\beta_s)$ and $\omega_s (= c\beta_s/R_s)$. Expanding ω to the first order in $\frac{\Delta\eta}{\eta_s}$ one obtains

$$\omega = \omega_s \left[1 + \Lambda \frac{\Delta\eta}{\eta_s} \right], \tag{3}$$

where

$$\Lambda = \frac{1}{\gamma_s^2} - \frac{1}{\gamma_t^2}$$

and γ_t is the transition energy in mc^2 units. The equations of motion now become

$$\begin{cases} \dfrac{d\phi}{dt} = \omega_{rf} - h\omega_s \left[1 + \dfrac{\Lambda}{\eta_s} \Delta\eta \right] & (4) \\[2ex] \dfrac{d(\Delta\eta)}{dt} = \dfrac{eV_{rf}}{mc^2} \dfrac{\omega_s}{2\pi} \dfrac{1}{\beta_s} \sin\phi - \dot{\eta}_s & (5) \end{cases}$$

where $\dot{\eta}_s(t) = d\eta_s/dt$.

Since $dn/dt = \omega/2\pi$ where n is the revolution number for the particle, the equations of motion can also be written as

$$\begin{cases} \dfrac{d\phi}{dn} = \omega_{rf} \dfrac{2\pi}{\omega_s} \left[1 - \dfrac{\Lambda}{\eta_s} \Delta\eta \right] - 2\pi h & (6) \\ \dfrac{d(\Delta\eta)}{dn} = \dfrac{eV_{rf}}{mc^2} \dfrac{1}{\beta_s} \sin\phi - \dfrac{2\pi}{\omega_s} \dot{\eta}_s \ . & (7) \end{cases}$$

In Eqs. (5) and (7), the expansions for ω and β stop at the zero-th order. Assuming that the changes of $V_{rf}(t)$, $\omega_{rf}(t)$, $\eta_s(t)$ and $\dot{\eta}_s(t)$ are small within one turn, the turn-by-turn integration for a particle becomes

$$\phi_{n+1} = \phi_n + \omega_{rf}(t_n) \left(\frac{2\pi}{\omega_s}\right)_n \left[1 - \frac{\Lambda_n}{\eta_s(t_n)} \Delta\eta\right] - 2\pi h, \tag{8}$$

$$(\Delta\eta)_{n+1} = (\Delta\eta)_n + \frac{eV_{rf}(t_{n+1})}{mc^2} \frac{1}{(\beta_s)_{n+1}} \sin\phi_{n+1} -$$

$$- \left(\frac{2\pi}{\omega_s}\right)_{n+1} \dot{\eta}_s(t_{n+1}), \tag{9}$$

where

$$t_{n+1} = t_n + \left(\frac{2\pi}{\omega_s}\right) n \ . \tag{10}$$

From Eqs. (4) and (5), the Hamiltonian of the system is

$$H(\psi, \Delta\eta, t) = \left(1 - \frac{\omega_{rf}}{h\omega_s}\right) \beta_s \Delta\eta + \frac{1}{2} \frac{\Lambda}{\gamma_s} (\Delta\eta)^2$$

$$- \frac{1}{2\pi h} \frac{eV_{rf}}{mc^2} \cos\phi - \frac{\beta_s}{h\omega_s} \dot{\eta}_s \phi \ . \qquad (11)$$

Equations (8) through (10) are the basis for the numerical integration. They represent the physical situation of a single accelerating gap in the ring. However, these equations are sufficiently good approximations for our purpose.

B. Parameters and Computation Procedure

The booster ring-magnet (15 Hz, biased-sinusoidal excitation) parameters are

$$\begin{cases} \gamma_t = 5.446 \\ R_s = 75.47 \text{ m} \\ \eta_s(t) = A - B \cos 15(2\pi t) \\ \qquad A = \frac{1}{2}\left[\eta(8 \text{ GeV}) + \eta(200 \text{ MeV})\right] = 5.08034 \\ \qquad B = \frac{1}{2}\left[\eta(8 \text{ GeV}) - \eta(200 \text{ MeV})\right] = 4.39349 \ . \end{cases} \qquad (12)$$

The rf parameters are specified as follows:

$$\begin{cases} h = 84 \\ V_{rf}(t) = \text{16 equal steps at 10 } \mu\text{sec/step ending in a total final voltage which is adjustable between 100 kV and 250 kV. The cases in which all 16 cavities are turned on simultaneously was also tried.} \\ \omega_{rf}(t) = \text{Different functions within the 160 } \mu\text{sec trapping time were tried. Most useful are linear functions with various slopes. For proper continuation into the acceleration cycle all frequency programs studied end up at the synchronous frequency } h\omega_s \text{ at the end of trapping.} \end{cases}$$

For the computation we first uniformly populate the $(\phi, \frac{\Delta\eta}{\eta})$ phase space with 1000 particles within a band having a $\frac{\Delta\eta}{\eta}$ width corresponding to the assumed initial momentum spread and extending from $\phi = -\pi$ to $\phi = \pi$. Two remarks should be noted for this initial distribution.

1. The 200 MHz bunching in the linac beam is ignored. Since the booster rf frequency of ~30 MHz is much lower than 200 MHz this is expected to be a good approximation.

2. The momentum distribution in the linac beam is closer to being parabolic rather than uniform. The assumed uniform distribution contains relatively too many particles at the edges of the distribution (large momentum deviations). The capture efficiency so obtained is likely to be an underestimate and should be considered as a lower limit.

With given V_{rf} and ω_{rf} programs the motion of each particle is traced using Eqs. (8), (9), and (10). At the end of trapping the rf bucket, namely the separatrix of the Hamiltonian given by Eq. (11), is calculated and plotted together with the phase points of the 1000 particles. The rf bucket plotted corresponds to a synchronous momentum gain $\dot{\eta}_s$ and an rf voltage V_{rf} both equal to their values at the end of trapping, and an rf frequency ω_{rf} tracking the synchronous frequency. Such a bucket can, therefore, serve as a measure of the capture efficiency at that instant - particles inside the bucket are considered captured. Of course, since $\dot{\eta}_s$ is still rapidly increasing if V_{rf} does not increase sufficiently rapidly to maintain the bucket area what is captured at the end of trapping may be lost later on. To keep all the "captured" particles the bucket area at the end

of trapping must, at the minimum, be maintained throughout the acceleration cycle.

C. Results and Discussions

1. As a "control" and a case of academic interest we ran the case in which η_s = const. = $\eta_s(t=0) \equiv \eta_{s0}$.

Initial momentum and spread: $\eta_i = \eta_{s0}(1 \pm 0.8 \times 10^{-3})$

Synchronous momentum: η_s = constant = η_{s0}

rf voltage: stepwise turn-on to 100 kV total

rf frequency: $\omega_{rf} = h\omega_s$ = synchronous value .

As expected this case of capture into truly stationary bucket gives 100% efficiency with negligible phase-space dilution. At the end of trapping the beam occupies about 70% of the bucket area as predicted analytically. The phase plot is shown in Fig. 1a.

2. In the present "normal" operation one tries to accomplish the following tuning:

Initial momentum and spread: $\eta_i = \eta_{s0}(1 \pm 0.8 \times 10^{-3})$

Synchronous momentum: $\eta_s = A - B \cos 30\pi t$

rf voltage: stepwise turn-on to 100 kV total

rf frequency: $\omega_{rf} = h\omega_s$ = synchronous value.

In this case the beam is accelerated to follow the synchronous momentum, hence to stay on the synchronous radius R_s = const. The capture efficiency drops to 88%. As mentioned in the introduction acceleration reduces the bucket area and causes filamentation in the phase space. The phase plot is shown in Fig. 1b.

3. Practically it is difficult to program the rf frequency to follow the synchronous value percisely throughout the 160 μsec trapping time. We ran the case in which ω_{rf} has the synchronous values at the beginning and the end of the trapping time but

varies linearly in time in between. Other parameters are identical to case 2 above:

Initial momentum and spread: $\eta_i = \eta_{s0}(1 \pm 0.8 \times 10^{-3})$

Synchronous momentum: $\eta_s = A - B \cos 30\pi t$

rf voltage: stepwise turn-on to 100 kV total

rf frequency: $\omega_{rf} = a + bt$ (= $h\omega_s$ at beginning and end of trapping time).

The capture efficiency drops further to 75%. The captured particles occupy less than 70% of the bucket araa. The phase plot is shown in Fig. 1c.

4. Much better capture efficiency can be obtained by eliminating the acceleration during capture. The beam is then captured into stationary buckets. This is approximated by injecting a beam at a higher momentum corresponding to $\eta_{sf} \equiv \eta_s(t = 160\ \mu sec)$ at the end of trapping, and tuning the rf frequency to the synchronous value $h\omega_{sf}$ at the end of trapping and keeping it constant during trapping. For exact no-acceleration the rf frequency should rise slightly during trapping but this proves to be indistinguishable from the constant-frequency case. The parameters are:

Initial momentum and spread: $\eta_i = \eta_{sf}(1 \pm 0.8 \times 10^{-3})$

Synchronous momentum: $\eta_s = A - B \cos 30\pi t$

rf voltage: stepwise turn-on to 100 kV total

rf frequency: $\omega_{rf} = h\omega_{rf}$ = constant.

The capture efficiency increases to 98%. The bucket filling factor is about 90% as shown in Fig. 1d. There is essentially no dilution in the phase space.

Other linear rf frequency programs with various slopes were

tried, but none was found to be better than this case of zero slope.

5. Again for academic interest the non-adiabatic capture with all 16 cavities turned on simultaneously was also investigated. With the frequency programs described above in cases 3 and 4 the capture efficiency is found to be 71% for both cases agreeing with analytical predictions. Figs. 2a and 2b show the phase plots corresponding to the linearly changing ω_{rf} and constant ω_{rf} respectively. The large scale filamentation is the result of the sudden turn-on.

6. The capture efficiency as a function of the final rf voltage in a stepwise turn-on was also studied. Results for an initial momentum spread of $\Delta\eta/\eta = \pm 0.8 \times 10^{-3}$ is shown in Fig. 3a where we follow the same frequency programs as in cases 3 and 4. It is interesting to observe that we need a final voltage of 200 kV to capture 98% of the beam when the linearly changing ω_{rf} is used. This is twice the voltage required for the case of constant frequency.

7. The calculation in case 6 is repeated for an initial momentum spread of $\Delta\eta/\eta = \pm 1.2 \times 10^{-3}$, which is a more realistic goal even with the addition of a debuncher. About 250 kV is required to capture 92% of the beam fortthe case of linearly changing rf frequency, while only 150 kV is needed for the case of constant frequency. The capture efficiencies are plotted in Fig. 3b.

In summary, this study shows that the proper tuning for capturing a beam with momentum spread $\pm 1.2 \times 10^{-3}$ is

a. Inject at a momentum equal to the synchronous momentum

at the end of trapping which is 1.00073 times that at the beginning of trapping.

b. Set the rf frequency equal to the synchronous frequency at the end of trapping and hold it constant during the entire trapping time. This frequency is 1.00049 times that at the beginning of trapping.

c. Stepwise turn on the rf cavities to a final total voltage of at least 175 kV.

d. Beyond the end of trapping the rf frequency should be modulated to track the synchronous frequency and the rf voltage should be programmed to, at least, maintain the rf bucket size at the end of trapping. Operating in this manner one should be able to obtain a close to 100% transmission through the booster.

References

1. J.A. MacLachlan, "RF Capture in the NAL Booster", NAL Report TM-303, (May 1971)

2. W.W. Lee, "Effects of Nonlinearities on the Phase Motion in the NAL Booster", NAL Report TM-333 (Dec. 1971)

3. A.G. Ruggiero, private communication.

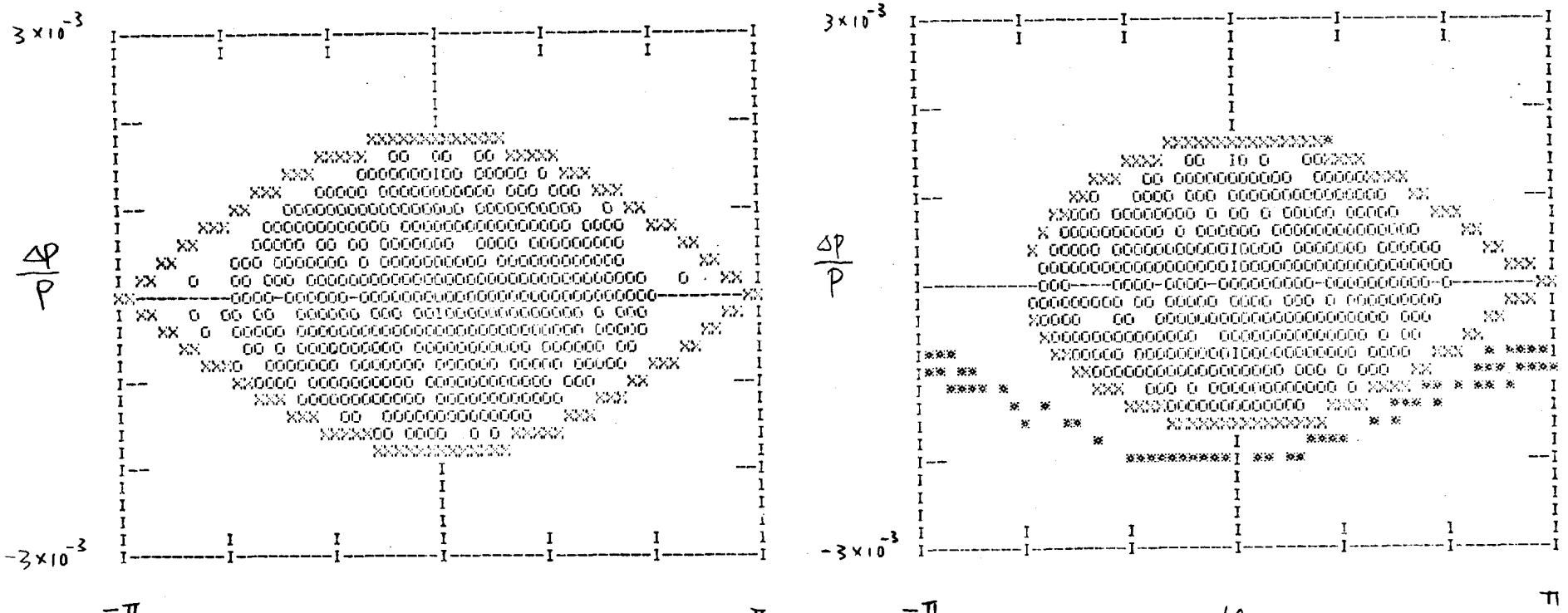

(a) no acceleration, $\omega_{rf} = h\omega_s$

(b) $\omega_{rf} = h\omega_s$

O .... captured particles

✱ .... lost particles

X .... seperatrix

Initial $\Delta p/p = \pm 0.8 \times 10^{-3}$, Final $V(t) = 100\ kV/turn$

Fig. 1 phase plots at the end of the capture for the stepwise turn-on

TM-473
0330

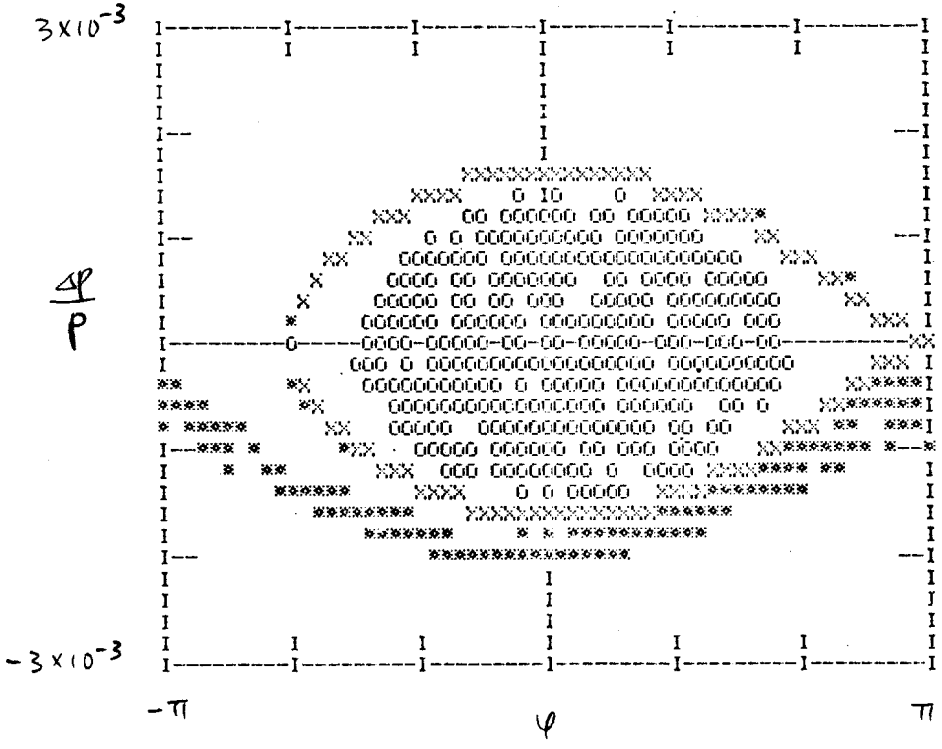

(c) $\omega_{rf} = a + bt$

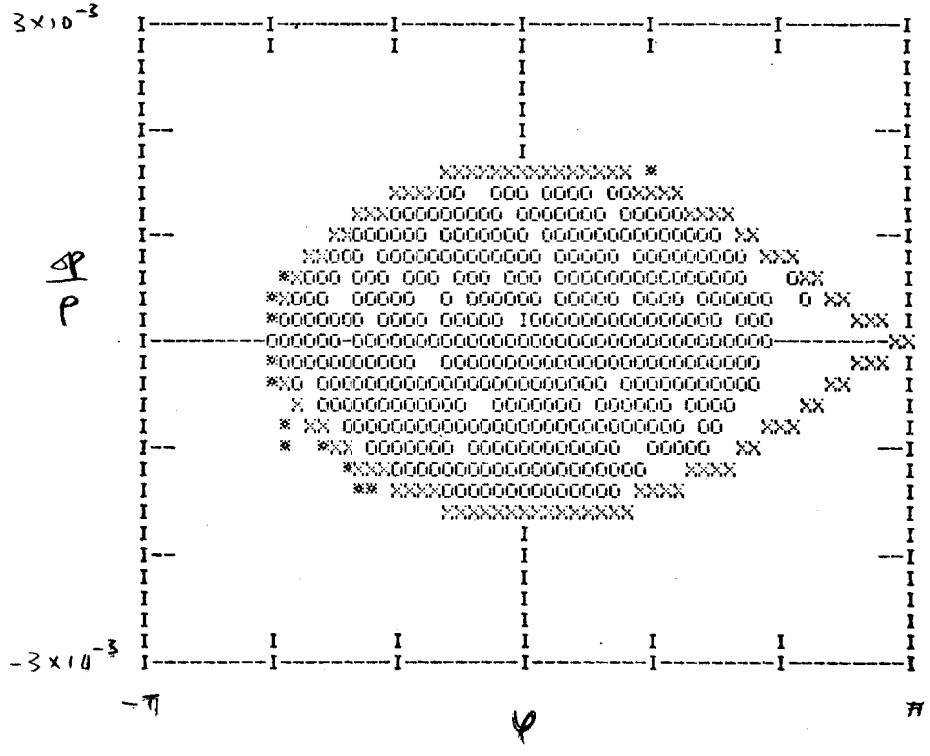

(d) $\omega_{rf} = c$

O ... captured particles

✱ ... lost particles

X ... seperatrix

Initial $\Delta p/p = \pm 0.8 \times 10^{-3}$, Final $V(t) = 100$ kV/turn

Fig. 1 (cont.) Phase plots at the end of the capture for the stepwise turn-on

TM-473
0330

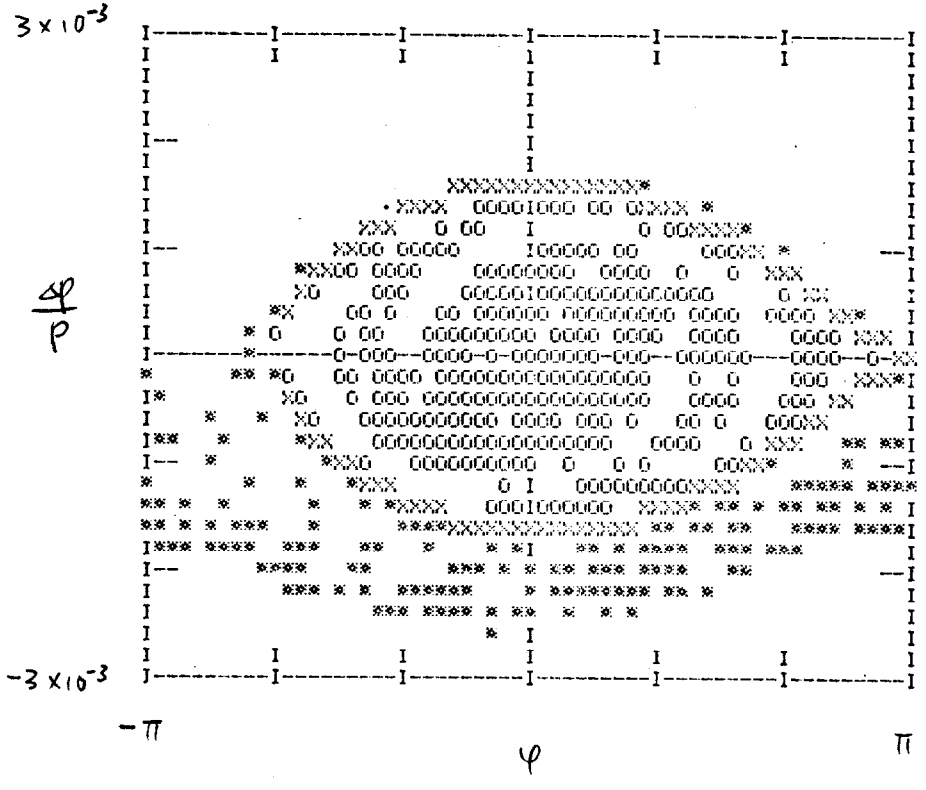

(a) $\omega_{rf} = a + bt$

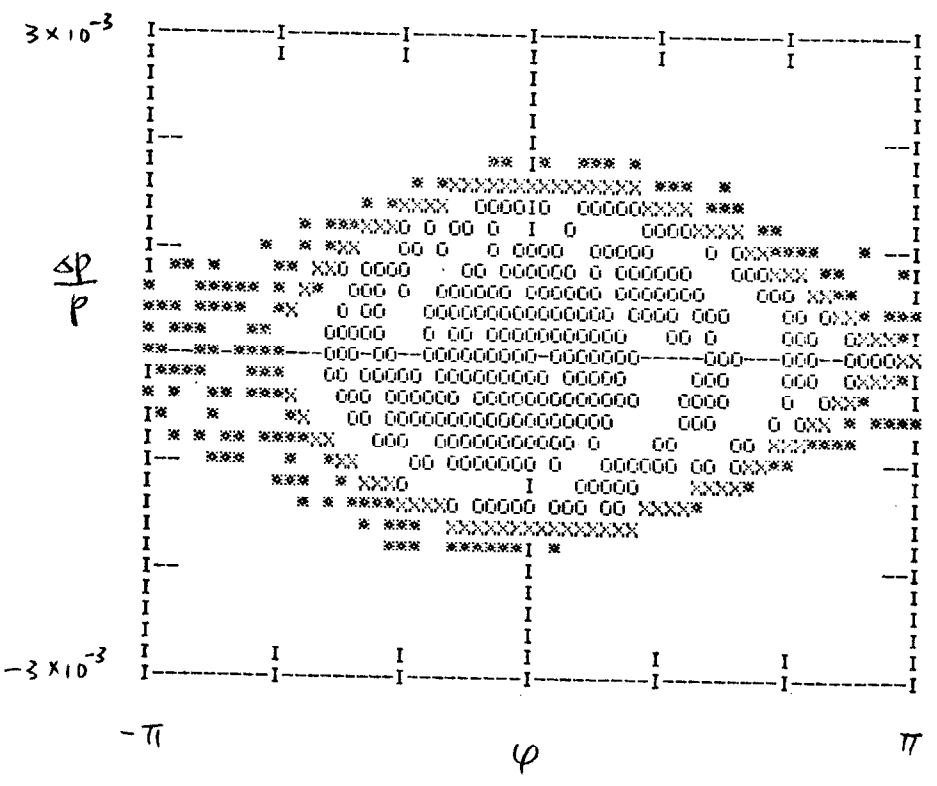

(b) $\omega_{rf} = c$

○ --- captured particles

✡ --- lost particles

X --- seperatrix

Initial $\Delta p/p = \pm 0.8 \times 10^{-3}$, Final $V(t) = 160$ kV/turn

Fig. 2 Phase plots at the end of the capture for the abrupt turn-on

TM-473
0330

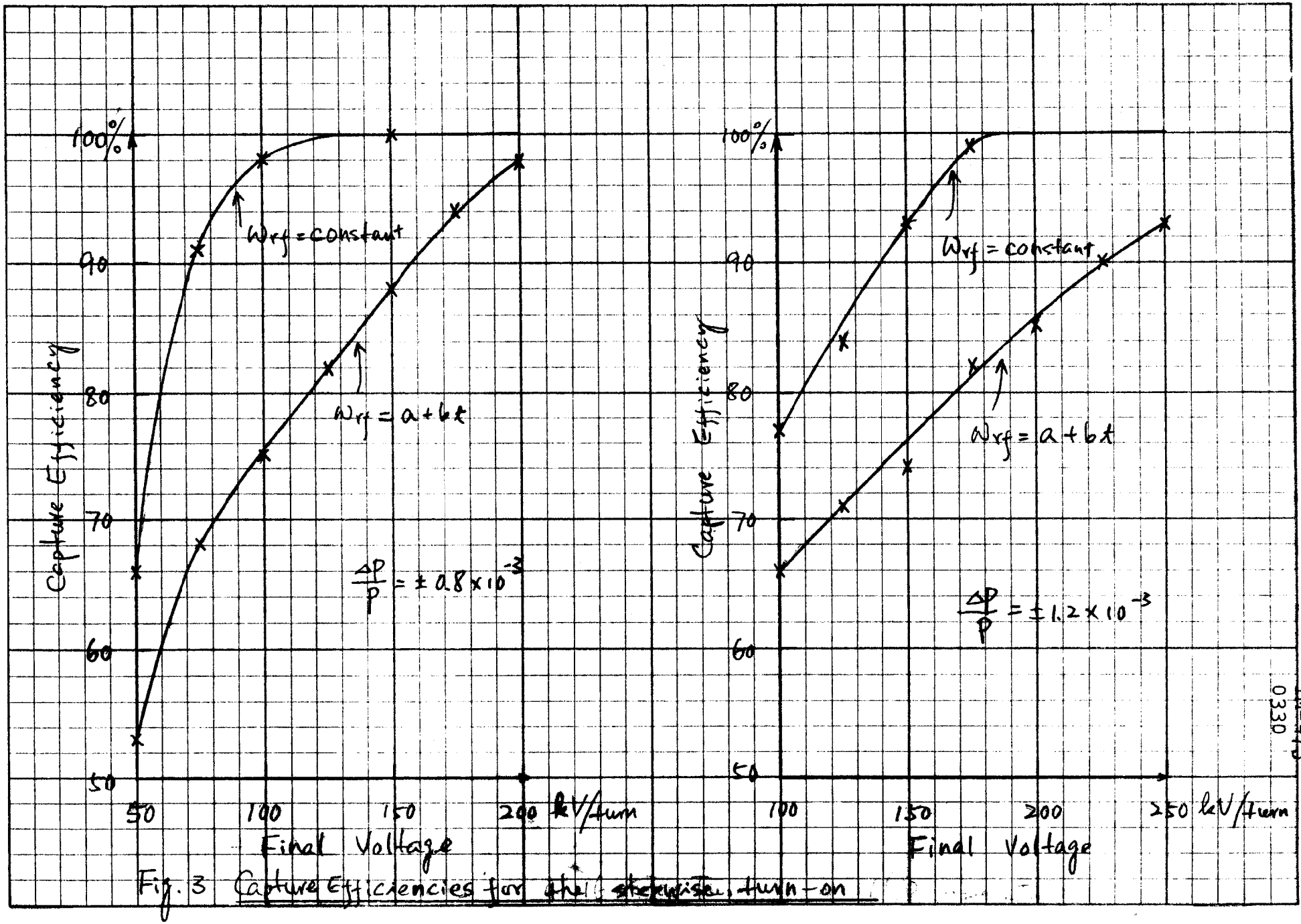

Fig. 3 Capture Efficiencies for the sinewise turn-on

TM-473
0330